Available online at www.sciencedirect.com
SCIENCE DIRECT®
Earth and Planetary Science Letters 243 (2006) 211–217
EPSL
www.elsevier.com/locate/epsl

Lithospheric elasticity promotes episodic fault activity

Jean Chéry [a,*], Philippe Vernant [b]

[a] Laboratoire Dynamique de la Lithosphère, CNRS-Université de Montpellier II, CC 060, place E. Bataillon, 34095 Montpellier Cedex 05, France
[b] Earth, Atmospheric and Planetary Sciences Department, Massachusetts Institute of Technology, 54-617, 77 Massachusetts avenue, Cambridge, MA 02139-4307, USA

Received 29 June 2005; received in revised form 13 December 2005; accepted 16 December 2005
Available online 2 February 2006
Editor: V. Courtillot

Abstract

Based on the agreement between geodetic and geological plate velocities, interplate fault slip rates are usually considered constant over long periods of time. However, measurements made at different time scales on intracontinental faults suggest that slip rate evolves with time. We examine the slip evolution of a fault embedded in an elastic lithosphere loaded by plate motion. We first assume that the fault friction varies due to a climatic cause. Then we show that high fault stress and low lithospheric stiffness favour large variations of slip rate. In the case where fault weakening is controlled by slip rate, we find that high loading velocity leads to a low stress, constant slip rate, while low loading velocity drives the fault slip rate to cycle between high and low values. This suggests that paleoseismic slip rate could overpass the loading velocity but also fall to zero for some period of time.

Keywords: fault; slip rate; elasticity; friction; lithosphare

1. Introduction

The slip rate of a fault corresponds to the ratio between displacement of fault sides and the elapsed time for this motion. Because fault slip rate is directly related to the repeat time of earthquakes rupturing the fault [1], its knowledge is critical for the assessment of seismic hazard. Both geodetic and geologic methods are used to determine slip rates. Geodetic measurements are based on the concept that the slip released by several earthquakes corresponds to a continuous crustal loading at some distance from the fault (typically 50 km for a large strike slip fault, see Savage and Prescott [2]). Using this concept, geodetic measurements during the interseismic period allow us to determine the fault slip rate [3]. Paleoseismic measurements done by trenching the fault plane provide the sequence of slip events due to the most recent earthquakes. Dating available markers constrains the slip rate over periods of between 100 and 10 000 yr. In the following, we call geodetic or paleoseismic slip rate estimates short term slip rate. In the landscape, the combination of climatic events and accumulated fault slip appears as morphotectonic features (stream deviations, moraine offsets) that can resist to erosion for more than 100 kyr [4]. These dated offsets features lead to long term slip rate estimates. Over longer time periods, structural geology allows to match the large displacement of dated

* Corresponding author.
E-mail address: jean@dstu.univ-montp2.fr (J. Chéry).

0012-821X/$ - see front matter © 2006 Elsevier B.V. All rights reserved.
doi:10.1016/j.epsl.2005.12.014

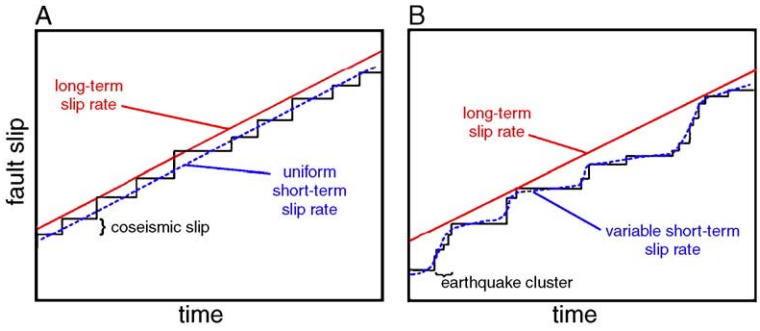

Fig. 1. Two kinds of seismic cycle models. A) quasi-periodic earthquake occurrence [45] leads to similar slip rate velocities for both geodetic (short term, dashed curve) and geologic (long term) estimates; B) clustered earthquake occurrence (Wallace's model) leads the slip rate to be time scale dependant. Short term slip rate (dashed curve) can be either smaller or larger than the geologic (long term) time scale.

geological bodies (e.g., lava flows, granitic plutons or sedimentary layers) and provide an estimate on the very long term (geologic) slip rate ($\sim 10^6$ yr).

Although only few faults have been extensively studied over these four time scales, a living paradigm is that slip rate does not evolve much during these time scales. This implies that fault motion at geodetic (10 yr) and geologic (10^6 yr) time scales should lead to a unique estimate (Fig. 1A). This idea is rooted into two observations. First, early comparisons between geodetic and morphotectonic slip rate on large faults such as the San Andreas lead to the same slip rates of ~34 mm/yr for the central segment of the San Andreas fault [5]. This value seems also true on a longer time scale as indicated by geological reconstructions [6]. Second, a good agreement occurs between the plate motion model derived from 1–3 Myr seafloor magnetic anomalies and the geodetic plate motion computed from GPS sites on land [7].

Conversely, the rapid increase of historical, geological and geodetic studies suggests that intracontinental earthquake related fault motion often occurs in a clustered manner (Fig. 1B) rather than by the accumulation of slip from periodic or quasi periodic earthquakes. Therefore, as suggested by Wallace [8], phases of intense activity are separated by long periods of quiescence [9–11]. The characteristic time between successive clusters seems to be highly variable, ranging from hundreds of years [12] to thousands of years [13] or even up to 30 kyr [9]. Moreover, some large intracontinental faults display a mismatch between geodetic and morphotectonic slip rates. In western US, the Wasatch fault in the Basin and Range presents an interseismic GPS slip rate of 3–4 mm/yr, while the slip rate falls to 0.5–1 mm/yr when larger time scales are taken into account [10]. Another example is the Altyn Tagh fault in Tibet. This very large intracontinental fault that may slip at a rate of 27±7 mm/yr according to morphotectonic analysis [4,14], while its geodetically determined velocity is estimated to 9±4 mm/yr [15] consistent with paleoseismic observations [16].

2. Model basics

Let assume a faulted lithosphere remotely loaded by a constant loading velocity. Different reasons have been given to explain why the fault slip may vary, all potentially related to fault strength variation. If two or more faults are present, their slip rates can co-vary [8] for the Basin and Range, and recently documented for the San Jacinto fault and the San Andreas fault in Southern California [17]. If only one fault is considered, then lithospheric elasticity must be advocated to explain a fault slip rate variation. In this case, deep postseismic viscous strain can be the source of crustal transient strain that in turn allows earthquake clustering [18,19]. Also, a hardening/softening friction model of the seismogenic zone allows the fault slip rate to vary [20]. We examine a one-fault mechanical model leading to a variable fault slip rate suggested by Wallace [8]. Let consider a tectonic system loaded by plate motion at a constant velocity. In this case, fault slip rate variation must correspond an to an equivalent strain change elsewhere in the lithosphere. To investigate how this behaviour could arise, we consider a wide lithospheric domain crossed by a large fault (Fig. 2A). Our inspiration here is the geometry of broad intracontinental domains such as western US or Tibet. The simplest idealization of this tectonic setting corresponds to 1D model made of a spring (the lithosphere) loaded at a known velocity V, while a slider (the fault) moves at an unknown slip rate S (Fig. 2B). Doing that, we do not account in the following for the geometrical factor of the fault displayed in the plan view model of Fig 2A. This

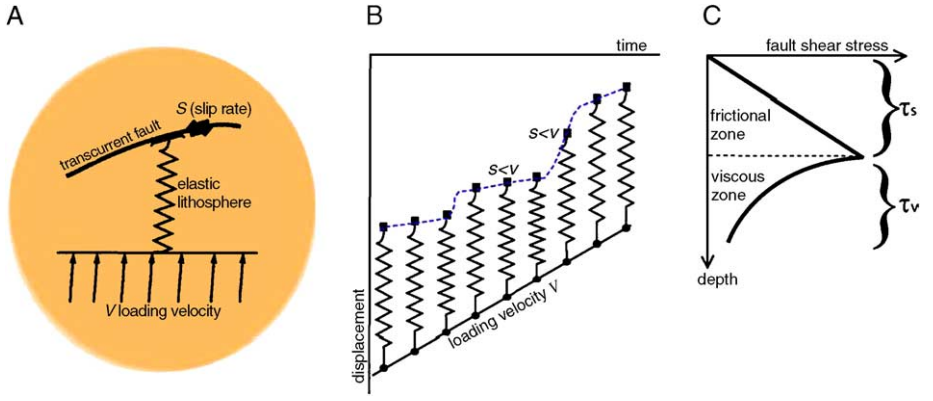

Fig. 2. A) Conceptual model of a large strike-slip fault embedded in a large continental domain inspired by the geodynamical framework of Tibet and of the Altyn–Tagh fault. B) A compliant lithosphere allows transient strain to occur according to variable fault friction. Therefore, fault slip rate S can vary under constant loading velocity. C) Rheological fault model in which the fault shear stress is the sum of frictional stress τ_s in the upper crust and of viscous stress τ_v in the lower crust.

would imply that the velocity S that we discuss in the following 1D model has to be divided by the sinus of the angle between the azimuth of driving velocity V and the azimuth of the fault to match the along fault velocity of Fig 2A. In order to study the fault slip rate evolution, we use stress balance that imposes the equality between lithospheric stress σ and fault stress τ. Average lithospheric stress at a time t is given by:

$$\sigma = k(V \cdot t - U) \quad (1)$$

where k is the lithospheric stiffness defined by the ratio of the Young's modulus E and the width of the intracontinental domain L. U is the cumulated slip fault given by $\int_0^t S\mathrm{d}t$. Following rheological models proposed for a weakly deformed continental crust [21], we postulate that average fault stress τ is the sum of a frictional stress τ_s occurring in the upper crust and of a thermally activated viscous stress τ_v operating in the lower crust (Fig. 2B). Our knowledge of crustal friction is based v on laboratory experiments and in situ stress measurements. Both indicate that shear stress rapidly increases with normal stress. Therefore, upper crustal stress seems to be controlled by high friction coefficient (0.6–0.8) and hydrostatic pore pressure. This typically leads to an average shear stress of about 100 MPa for the upper crust. A different behaviour is believed to exist on large interplate faults such as the San Andreas fault and for subduction boundaries. For those regions, direct stress estimates [22], stress retrieved from heat flow budgets [23] and geodynamical stress modelling [24,25] lead to average shear stress within 0–20 MPa. A plausible physical explanation for such a low stress is that high pore fluid pressure occurs in the fault core, inducing low effective pressure and therefore low shear stress [26]. Stress measurements close to active intracontinental faults lead to contrasted results. In situ stress measurements in slowly deforming areas such as Dixie Valley in the Basin and Range suggest high shear stress [27]. However, low shear stress has been deduced from curved striations on the small Nojima intraplate fault [28]. For deep fault zones, laboratory data suggest that viscous behaviour occurs by temperature dependent processes and non linear viscosity [29]. For sake of simplicity, we assume that the deep fault strength is controlled by a shearing flow along the fault direction with a characteristic width W. This ductile fault zone has a linear viscosity η and has a linear velocity variation S across W equal to the velocity jump occurring at the surface. Therefore, we assume that no horizontal shear occurs between the frictional part and the viscous part of the crust. According to this view, viscous stress is controlled by a material parameter $\eta_w = \eta / W$ and is given by:

$$\tau_v = \eta_W \cdot S \quad (2)$$

As a whole, the fault stress τ is the sum of a stabilising factor (the viscous stress increases with the slip rate) and of a potentially destabilising frictional term if $\frac{\partial \tau_s}{\partial t} < 0$.

3. Climate control

In the following, we assume that fault friction may evolve with time. We first explore the idea that climatic changes lead to environmental perturbation of a fault system. This may correspond to crustal water content variations or stress change caused by erosion–deposition processes as attested to by morphotectonic

and sedimentary observations. For sake of simplicity, we assume a cyclic variation leading the frictional stress:

$$\tau_s = \tau_0 + \Delta\tau \sin\frac{2\pi}{T}t \tag{3}$$

where τ_0 is the average shear stress on the fault plane, $\Delta\tau$ the stress change amplitude, and T the period of climatic variation. This non-linear mechanical system has two distinct dynamical behaviours. If crustal stress σ does not reach the frictional stress τ_s, then the fault is locked ($\sigma<\tau_s, S=0,\ \tau_v=0$). During this period, elastic stress accumulates at a rate $\dot{\sigma}=kV$. When the frictional stress is at yield τ_s, then S must balance the equation given by $\sigma=\tau_s+\tau_v$. Using the first derivative of stress balance, we obtain the following equation:

$$S + \frac{\eta_w}{k}\dot{S} = V - \frac{T\cdot\Delta\tau}{2\pi k}\cos\left(\frac{2\pi}{T}t\right). \tag{4}$$

Assuming an initial value of $U=0$ for $t=0$, numerical solutions are easily computed. Moreover, the analytical solution is tractable when $S>0$. Given that $\omega=2\pi/T$, $A=\eta_W/k$ and $B=\omega\cdot\Delta\tau/k$, slip rate is given by:

$$S = \frac{-B}{1+\omega^2A^2}\left[\omega A\cdot\sin(\omega t) + \cos(\omega t)\right] + V \tag{5}$$

In order to understand the gross physical meaning of the solution, we first neglect viscous stress τ_v. Then, the amplitude of slip rate change ΔS is simply:

$$\Delta S = 2\pi\frac{\Delta\tau}{T\cdot k}. \tag{6}$$

In the case of a broad intracontinental domain of 1000 km of extent, the stiffness of the model is 10^5 Pa/m if a Young modulus of 10^{11} Pa is assumed. The remaining variables are the climatic period and the stress change amplitude. As illustrated by Fig. 3A, a major issue is the magnitude of admissible stress change $\Delta\tau$. For the purpose of this discussion, we assume that the frictional stress is controlled by the Coulomb friction and that is equal to $C+\mu\cdot[\sigma_n-P]$, in which C is the cohesion and μ the intrinsic friction. Therefore, frictional stress variation may occur according to change of the normal stress σ_n and of the pore pressure P. If we suppose that climatic forcing induces cyclic formation of an ice cap, this will directly affect the fault normal stress as proven by mechanical modelling [30]. For example, a thickness of 100 m will cause a vertical stress variation of ~1 MPa impacting normal stress and in turn maximum sustainable shear stress on the fault plane. The pore pressure can also have a large effect on the fault strength [26]. If we assume that pore pressure can vary between hydrostatic to lithostatic values, then effective normal stress change are on the order 100 MPa at 10 km depth. Despite that the connection between the surface hydrological cycle and the deep fluids in fault is not well known, hydrological signature of earthquakes are clear, attesting the large scale permeability of the crust. Therefore, shear stress variation in the range of [0.1–10 MPa] induced by climate impact on crustal loading and pore pressure change seems possible. A change of 1 MPa would correspond to only 1% of the sustainable frictional stress by a strong fault. Slip rate change of 6 and 0.6 mm/yr are predicted for periods of 10 and 100 kyr, respectively. Larger stress changes lead to slip rate changes larger than the loading velocity, causing the fault to stop. For example, a climatic period $T=10$ kyr, a stress change $\Delta\tau$ of 5 MPa and a loading velocity of 2 cm/yr leads the slip rate to vary between 0 and 5 cm/yr, as shown by Fig. 3B. These oscillations are partially damped if viscous stress is accounted for. Using a fault zone viscosity of 10^{19} Pas deduced from

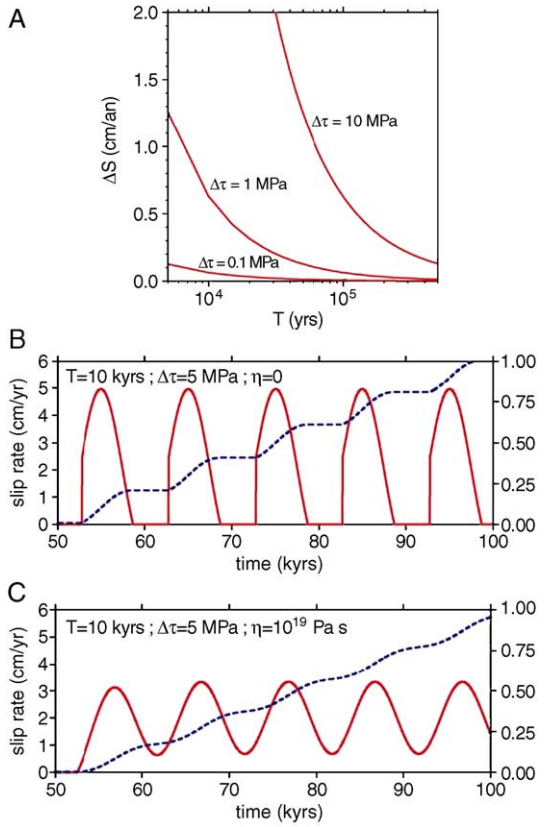

Fig. 3. A) Amplitude of slip rate variation with respect to stress change periodicity (5–500 kyr) for stress change amplitudes of 0.1, 1 and 10 MPa. B) Slip rate variation (solid line) and cumulated slip (dashed line) with $\eta=0$. C) Slip rate variation (solid line) and cumulated slip (dashed line) with a viscous damping corresponding to $\eta=10^{19}$ Pas.

geodetic studies [31] and a deep fault zone width of 1 km allows a significant part of the fault stress to be taken by viscous process, but still large slip rate oscillation occurs (Fig. 3C).

4. Strain softening/hardening

We now investigate the idea that effective fault friction occurs thanks to a velocity weakening process. Up to now, a connection between effective friction and velocity or slip has mostly been advocated to explain seismic motion. Indeed, rate and state friction laws reproduce well the phenomenon of dry friction, including slip rate weakening and self healing [32,33]. Here we adopt a similar model, but applying it to geological time scales. We assume a simple law presenting a linear decay of the frictional stress from τ_0 up to a constant value τ_1. We also hypothesize that the weakening process does not happen instantaneously, but is due to repeated earthquakes, leading fault to gradual softening or strengthening [20,34]. Therefore, we introduce an average slip rate $\bar{S} = \int_{t-T_w}^{t} S\mathrm{d}t$ which controls our ad hoc friction law:

$$\tau_s(t) = \max\left[\tau_0\left(1-\frac{\bar{S}}{S_0}\right); \tau_1\right] \quad (7)$$

where the slip rate weakening parameter S_0 and the weakening time T_w controls the weakening process. Such an equation provides a convenient rheological model explaining why slow or inactive faults are strong, whereas rapidly slipping faults work at low stress. Solving leads to the following first order equation:

$$S + \frac{1}{k}\left(\eta_W + \frac{\partial \tau_s}{\partial S}\right)\dot{S} = V. \quad (8)$$

Such an equation has an exponential solution decaying towards V if its characteristic time scale $t_C = -\frac{1}{k}\left(\eta_W + \frac{\partial \tau_s}{\partial S}\right)$ is negative, meaning tha $\frac{\partial \tau_s}{\partial S} > -\eta_W$. Using parameters similar to those used in the for climatic variation experiments, we test a weakening law with $\tau_1 = 10$ MPa, assuming that this low stress occurs when the long term slip rate exceeds 5 cm/yr (as for most of subduction zones). This weakening law is consistent with the assumption that slow faults are strong, whereas fast fault becomes weak. Because of the dependence of $\frac{\partial \tau_s}{\partial S}$ on S and T_w, the stress balance cannot be evaluated by analytical means. We search numerically for how the loading velocity V and the weakening time T_w controls the slip rate over 300 kyr. When the loading rate is high ($V = 8$ cm/yr), the solution unconditionally converges towards a constant fault slip rate ($S = V$) in a zone where the dynamical system is stable $\left(\frac{\partial \tau_s}{\partial S} = 0\right)$. A loading velocity of 2 cm/yr causes the slip rate to cycle if the weakening time is lower than 35 kyr (Fig. 4A). In this case, the fault stress τ evolves between 100 and 20 MPa, while the viscous stress τ_v acts by limiting the slip rate (Fig. 4B). For such a periodic behaviour, the short term slip rate evolves between 0 and 6 cm/yr (Fig. 4C), providing no valuable information about the long term slip of the fault. Weakening times larger than 35 kyr lead oscillations that slowly damp towards the loading velocity.

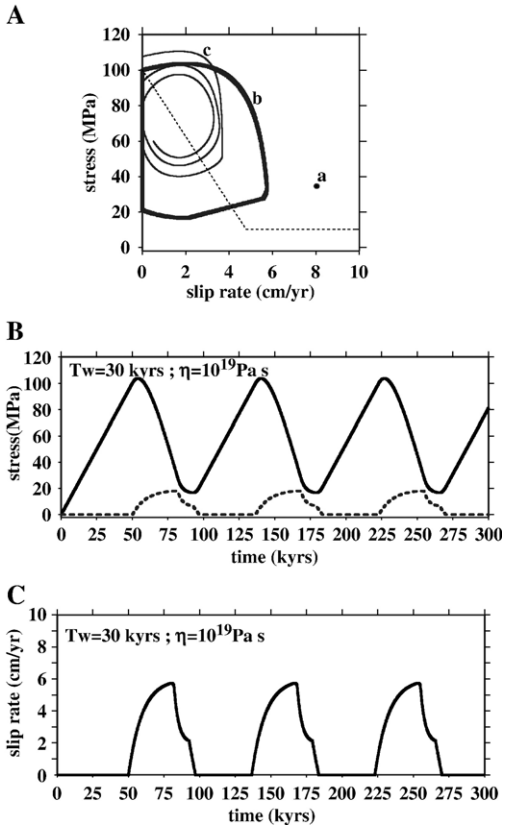

Fig. 4. A) Stress slip rate evolution of the slip rate weakening system for two loading velocities (2 and 8 cm/yr) and for 2 weakening times (30 and 40 kyr). Velocity of 8 cm/yr always leads to constant slip rate (a). A moderate loading velocity leads to a periodic attractor ($T_w = 30$ kyr, curve b) or progressively damp ($T_w = 40$ kyr, curve c). B) Stress evolution for case (b) (total fault stress in solid line and viscous stress in dashed line). C) Slip rate evolution of case (b) displaying episodic fault behaviour.

5. Conclusions

The 1D model we have developed is too simple to account for the real geometrical and rheological complexities of the lithosphere. Nevertheless, it explains why

the activity of continental faults may strongly vary while plate motion remains constant. The basic ingredient for episodic fault activity is provided by a compliant lithosphere in which fault stress fluctuation can occur. In this respect, a large distance between the fault zone and the source of motion magnifies the ratio between slip rate variation and stress fluctuation as shown by Eq. (6). External and internal forcing can be a source of fault stress variation. For both cases, our modeling suggests that the ratio between fault slip rate variation (ΔS) and loading velocity (V) could be more important for continental faulting than for subduction faults. First, continental faults are loaded at smaller velocities than the plate boundary domains. Therefore, the relative slip rate change $\Delta S/V$ can more easily become larger than one, causing the fault to stop. Also, if we assume that continental faults are strong ($\tau_0 = 100$ MPa), their potential stress variation can be more important than those of a subduction zone faults which may correspond to a weak fault plane. Finally, it can be conjectured that climatic change affects predominantly the mechanical properties of continental faults [30] because of the direct interaction between the atmosphere and the crust, while water screening may limit climatic impact for subduction zones.

Among other possible causes for stress variation, a self-induced weakening/healing could be also efficient. If the weakening time is small enough, fast slip rate excursions occur, as well as a complete lack of activity. If this happens in nature, we should sometimes observe fault slip rates that are higher than plate loading ($S >> V$). Such observations have rarely been documented, but Weldon et al. have shown that the paleoseismic slip rate of the San Andreas fault may have reached 89 mm/yr over a 300 yr period [35], 3 times larger that the long term slip rate. An opposite behaviour, i.e., $S << V$, has been also reported as for example the Altyn Tagh fault in Tibet. In this case, the geodetic slip rate (9 mm/yr) is lower than the long term slip rate (27 mm/yr). This would mean that the Altyn Tagh strength is now increasing. Meanwhile, the strain provided by plate loading is stored elastically in the Tibetan lithosphere which in turn delays the time needed for the Altyn Tagh fault to rupture.

This behaviour provides a mechanical explanation of the Wallace's model (Fig. 1B). It could have deep implications on the real significance of the geodetic measurements on continents. If the geodetic velocity field is measured during an earthquake cluster, then the measured geodetic strain, corrected for interseismic motion could appear more localized (implying that $S > V$).

Despite no clear evidence of such behaviour is known, the North Anatolian fault could be in a high fault activity period. Indeed, this fault system is now in a clustered phase of earthquakes since 1939 [12], and the long term fault slip rate is slightly lower (18 ± 3.5 mm/yr, [36–38]) than the short term fault slip rate (24 ± 2 mm/yr, [39]). However, the uncertainties are such that both short and long term fault slip rates remain consistent and more accurate estimations need to be done to definitely conclude. By contrast, a GPS velocity field established during a period of low fault activity (anti-cluster) could show a rather continuous strain due to the transient strain accumulation in the lithosphere. This is perhaps the case now in Tibet as suggested by wide scale GPS surveys [40]. If this strain rate pattern is not representative of the long term, steady state process, geodetic measurements alone cannot be used to claim that the surface geological strain is driven by the lower crust or mantle flow [41]. The intermediate case corresponds to a quasi-constant earthquake recurrence time interval and a good agreement between long and short term fault slip rates. This is the case of the Dead Sea fault where $M > 7$ earthquakes are occurring with a 10 000 yr recurrence time interval since the last cluster of large earthquakes (some 50 000 yr ago [42]). Short term (4.3 ± 1 mm/yr, [43]) agree with the Late Pleistocene geomorphologic rate estimates (4 ± 2 mm/yr [44]).

Therefore, the respective use of long term and short term slip rates on continental faults must be clearly separated. Morphotectonic slip rates are chiefly useful to assess the style of tectonic deformation but does not provide relevant information on the fault hazard. On the other hand, paleoseismic slip rates and geodetic motion accurately monitor seismic hazard, but should not be directly used to validate long term geodynamical models.

Acknowledgements

We thank X. Le Pichon and S. McClusky for their useful comments on the early version of manuscript, and an anonymous reviewer that helped us to clarify the presentation of the mechanical model.

References

[1] G.C.P. King, R.S. Stein, J.B. Rundle, The growth of geological structures by repeated earthquakes: 1. Conceptual framework, J. Geophys. Res. 93 (1988) 13307–13318.
[2] J.C. Savage, W.H. Prescott, Asthenosphere readjustment and the earthquake cycle, J. Geophys. Res. 83 (1978) 3369–3376.
[3] M. Lisowski, J.C. Savage, W.H. Prescott, The velocity field along the San Andreas fault in central and southern California, J. Geophys. Res. 96 (1991) 8369–8389.
[4] P. Tapponnier, et al., Long-term slip rates and characteristic slip: keys to active fault behaviour and earthquake hazard, C. R. Acad. Sci., Sér. 2, Sci. Terre Planètes 333 (2001) 483–494.

[5] W. Thatcher, Present-day crustal movements and the mechanics of cyclic deformation, in: R.E. Wallace (Ed.), The San Andreas Fault system, California, Geological Survey Professional Paper: Washington, 1990, pp. 189–205.
[6] W.R. Dickinson, B.P. Wernicke, Reconciliation of San Andreas slip discrepancy by a combination of interior Basin and Range extension and transrotation near the coast, Geology 25 (1997) 663–665.
[7] G.F. Sella, T.H. Dixon, A. Mao, REVEL: a model for recent plate velocities from space geodesy, J. Geophys. Res. 107 (B4) (2002), doi:10.1029/2000JB000033.
[8] R.E. Wallace, Grouping and migration of surface faulting and variations in slip rates on faults in the Great Basin province, Bull. Seismol. Soc. Am. 77 (1987) 868–876.
[9] S. Marco, M. Stein, A. Agnon, Long term earthquake clustering: a 50,000-year paleoseismic record in the Dead Sea Graben, J. Geophys. Res. 101 (1996) 6179–6191.
[10] A.M. Friedrich, et al., Comparison of geodetic and geologic data from the Wasatch region, Utah, and implications for the spectral character of earth deformation at period of 10 to 10 million years, J. Geophys. Res. 108 (B4) (2003), doi:10.1029/2001JB000682.
[11] J.F. Ritz, et al., Slip rates along active faults estimated with cosmic-ray-exposure dates; application to the Bogd Fault, Gobi–Altai, Mongolia, Geology 23 (1995) 1019–1022.
[12] R.S. Stein, A.A. Barka, J.H. Dieterich, Progressive failure on the North Anatolian fault since 1939 by earthquake stress triggering, Geophys. J. Int. 128 (1997) 594–604.
[13] J. Chéry, S. Carretier, J.-F. Ritz, Postseismic stress transfer explains time clustering of large earthquakes in Mongolia, Earth Planet. Sci. Lett. 194 (1–2) (2001) 277–286.
[14] A.S. Mériaux, et al., Rapid slip along the central Altyn Tagh Fault: morphochronologic evidence from Cherchen He and Sulamu Tagh, J. Geophys. Res. 109 (B06401) (2004), doi:10.1029/2003JB002558.
[15] K. Wallace, Y.G. Bilham, R. Bilham, Inescapable low slip on the Altyn Tagh Fault, Geophys. Res. Lett. 31 (2004) L09613, doi:10.1029/2004GL019724.
[16] Z. Washburn, et al., Late Holocene earthquake history of the central Altyn Tagh Fault, China, Geology 29 (2001) 1051–1054.
[17] R. Bennett, A.M. Friedrich, K.P. Furlong, Codependent histories of the San Andreas and San Jacinto fault zones from inversion of fault displacement rates, Geology 32 (2004) 961–964.
[18] B.J. Meade, B.H. Hager, Viscoelastic deformation for a clustered earthquake cycle, Geophys. Res. Lett. 31 (L 10610) (2004), doi:10.1029/2004GL019643.
[19] S. Kenner, P. Segall, Time-dependence of the stress shadowing effect and its relation to the structure of the lower crust, Geology 27 (2) (1999) 119–122.
[20] Y. Ben-Zion, et al., Self-driven mode switching of earthquake activity on a fault system, Earth Planet. Sci. Lett. 172 (1999) 11–21.
[21] W.F. Brace, D.L. Kohlstedt, Limits on lithospheric stress imposed by laboratory experiments, J. Geophys. Res. 85 (1980) 6248–6252.
[22] M.D. Zoback, et al., New evidence on the state of stress of the San Andreas fault system, Science 238 (1987) 1105–1111.
[23] A.H. Lachenbruch, J.H. Sass, Heat flow and energetics of the San Andreas fault zone, J. Geophys. Res. 85 (1980) 6185–6222.
[24] J. Chéry, M.D. Zoback, R. Hassani, An integrated mechanical model of the San Andreas Fault in central and northern California, J. Geophys. Res. 106 (B10) (2001) 22,051–22,066.
[25] P. Bird, J. Baumgardner, Fault friction, regional stress, and crust mantle coupling in Southern California from finite elements models, J. Geophys. Res. 84 (1984) 1932–1944.
[26] J.R. Rice, Fault stress states, pore pressure distributions, and the weakness of the San Andreas Fault, in: B.E.a.T.-F. Wong (Ed.), Fault Mechanics and Transport Properties of Rock, Academic, San Diego, Calif., 1992, pp. 475–503.
[27] S.H. Hickman, et al., In situ and fracture permeability along the Stillwater fault zone, Dixie Valley, Nevada, Int. J. Rock Mech. Min. Sci. 34 (1997) 1–10.
[28] P.A. Spudich, et al., Use of fault striations and dislocation models to infer tectonic shear stress during the 1995 Hyogo-ken Nanbu (Kobe) earthquake, Bull. Seismol. Soc. Am. 34 (88) (1998) 413–427.
[29] S.H. Kirby, Rocks mechanics observations pertinent to the rheology of the lithosphere and the localization of strain along shear zones, Tectonophysics 119 (1985) 1–27.
[30] R. Hetzel, A. Hampel, Slip rate variations on normal faults during glacial–interglacial changes in surface loads, Nature 435 (2005) 81–84.
[31] W. Thatcher, Nonlinear strain buildup and the earthquake cycle on the San Andreas Fault, J. Geophys. Res. 88 (1983) 5893–5902.
[32] C.H. Scholz, Earthquakes and friction laws, Nature 391 (1998) 37–42.
[33] J. Dieterich, A constitutive law for rate of earthquake production and its application to earthquake clustering, J. Geophys. Res. 99 (1994) 2601–2618.
[34] N.H. Sleep, M.L. Blanpied, Creep, compaction, and the weak rheology of major faults, Nature 359 (1992) 687–692.
[35] R.J. Weldon, T. Fumal, G. Biasi, Wrightwood and the earthquake cycle: what a long recurrence record tells us about how fault work, GSA Today 14 (2004), doi:10.1130/1052-5173.
[36] R. Armijo, et al., Westward propagation of the North Anatolian Fault into the northern Aegean: timing and kinematics, Geology 27 (3) (1999) 267–270.
[37] A. Hubert-Ferrari, et al., Morphology, displacement, and slip rates along the North Anatolian fault, Turkey, J. Geophys. Res. 107 (2002), doi:10.1029/2001JB000393.
[38] A.-S. Provost, J. Chéry, R. Hassani, 3D mechanical modeling of the GPS velocity field along the North Anatolian fault, Earth Planet. Sci. Lett. 209 (2003) 361–377.
[39] S.M. McClusky, et al., GPS constraints on plate motions and deformations in eastern Mediterranean and Caucasus, J. Geophys. Res. 105 (2000) 5695–5719.
[40] Q. Wang, et al., Present-day crustal deformation in China by Global Positioning System measurements, Science 294 (2001) 574–577.
[41] P. England, P. Molnar, Active deformation of Asia: from kinematics to dynamics, Science 278 (1997) 647–650.
[42] Z.B. Begin, et al., A 40,000 year unchanging seismic regime in the Dead Sea rift, Geology 33 (4) (2005) 257–260.
[43] S. Mahmoud, R. Reilinger, S. McClusky, P. Vernant, Ali Tealeb, GPS evidence for northward motion of the Sinai Block: implications for E. Mediterranean tectonics, Earth Planet. Sci. Lett. 238 (2005) 217–224.
[44] Y. Klinger, et al., Slip rate on the Dead Sea transform fault in northern Araba Valley (Jordan), Geophys. J. Int. 142 (3) (2000) 755–768.
[45] K. Shimazaki, T. Nakata, Time-predictable recurrence model for large earthquakes, Geophys. Res. Lett. 7 (1980) 279–282.